



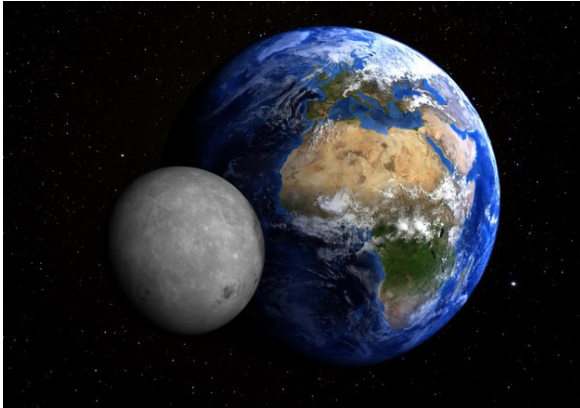
IASI instruments inter-comparisons and absolute calibration based on Moon acquisitions

Laura Le Barbier (CNES), Elsa Jacquette (CNES), Bojan Sic (NOVELTIS), Bernard Tournier (SPASCIA),
Yannick Kangah (SPASCIA), Emmanuel Dufour (NOVELTIS), Laurence Buffet (CNES), Mathilde Failot (CNES),
Oliver Vandermarcq (CNES), Jean-Christophe Calvel & Claire Baqué (AKKA)

Lunar Calibration Workshop, November 18th 2020



Contents



1. Study purposes
2. Overview of IASI moon acquisitions until now
3. Study conclusions
4. IASI moon acquisitions operational constraints
5. Upcoming program for the next phase of this study in 2021

1. Study purposes

❖ Moon acquisitions as a potential source for radiometric calibration in the TIR domain :

- To perform inter-comparison between TIR instruments (relative inter-calibration);
- To check the over-time radiometric calibration stability;
- For absolute calibration \Rightarrow trying a new calibration method for TIR using the Moon
The Moon is already used in VIS and SWIR (Pléiades, SEVIRI on MSG, MVIRI on MET7, VIIRS on NPP, HIRS on METOP...);

❖ IASI is considered as a reference for radiometric calibration for IR sounders (GSICS)

- Absolute radiometric calibration $< 0,5 \text{ K @}280\text{K}$
- Inter-comparisons between sounders $< 0,2 \text{ K @}280\text{K}$, nevertheless inter-comparisons between IASI using EW acquisitions are not perfect \Rightarrow Difficulties to discriminate the impact of the selected scenes from radiometric calibration defect

❖ Why using the moon as a source:

- No atmosphere on the Moon \Rightarrow spectrum close to flat, easier to calibrate the complete spectrum;
- Moon evolves in a predictable way depending on the Sun-Moon-satellite geometry \Rightarrow stable spectra between several successive visit from all IASI

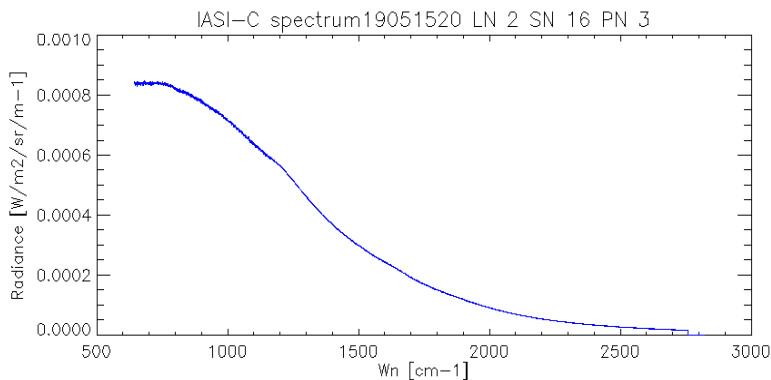
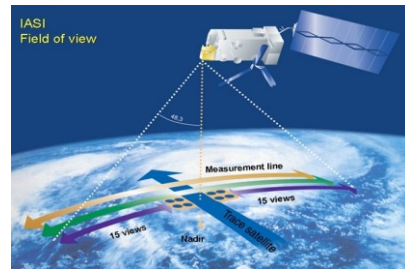
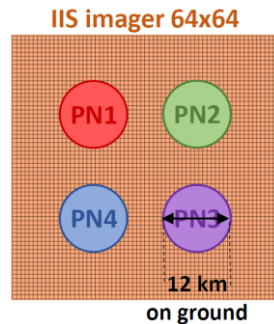
❖ Conduct of the first phase of the Moon study in 2019 :

Collaboration between CNES and NOVELTIS, with the help of EUMETSAT to plan the operations

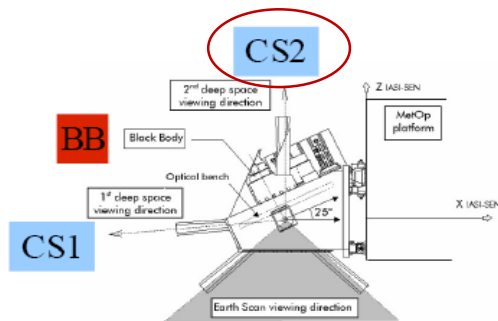
2. Overview of IASI moon acquisitions until now (1/4)

❖ How Moon acquisitions are performed with IASI (Fourier Transform Spectrometer + Imager IIS):

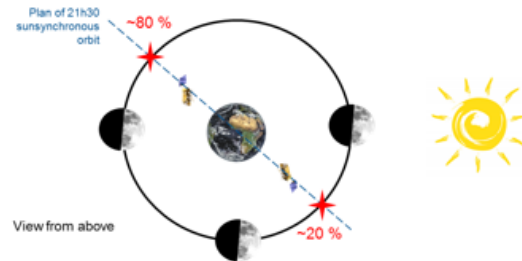
- A. A dedicated coding table was created and adapted to the moon's dynamics;
- B. Using a dedicated external calibration on Cold Space view CS2;
- C. The Moon is acquired once a month when its phase is at its maximum:



A. IASI-C Moon spectrum



B. IASI calibration views



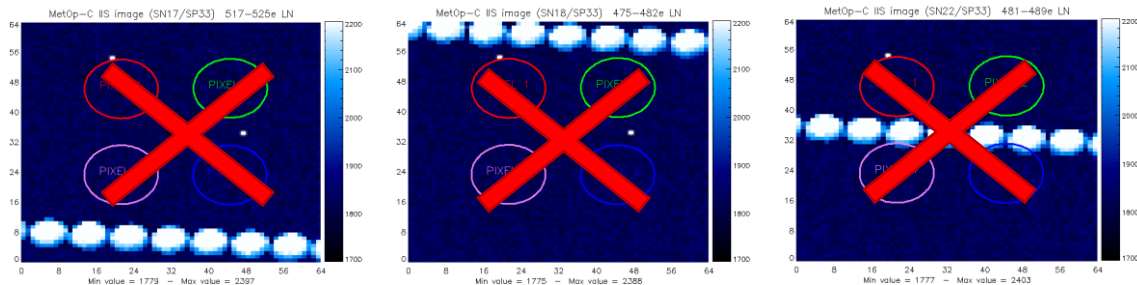
C. Maximum moon's phases

2. Overview of IASI moon acquisitions until now (2/4)

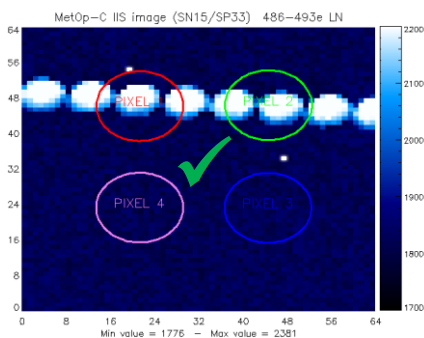
❖ Only 5 External calibration dedicated to Moon acquisitions in 2019 :

- May 15th : on IASI-C
- June 14th : on IASI-C
- July 13th-14th : on IASI-C
- August 12th : on IASI-C & IASI-B
- September : No acquisitions
- October 10th : on IASI-C & IASI-B

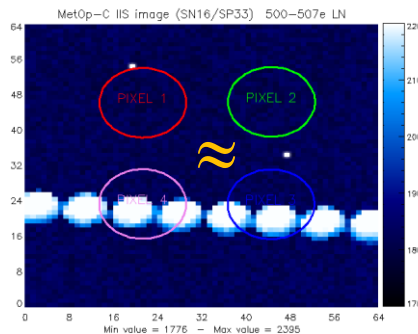
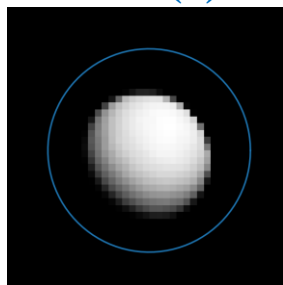
Example of the Moon transit seen in the IIS during one external calibration



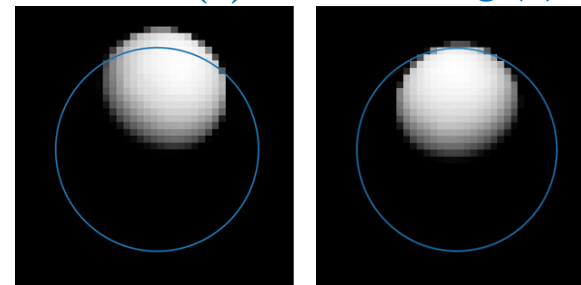
Different types of moon transit inside IASI pixel



Central (P) ✓

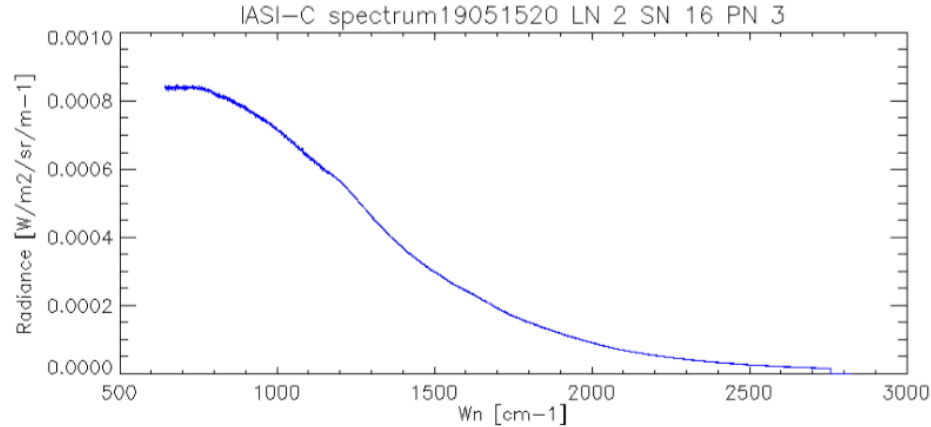


Partial (P) ≈ Bordering (L) ≈

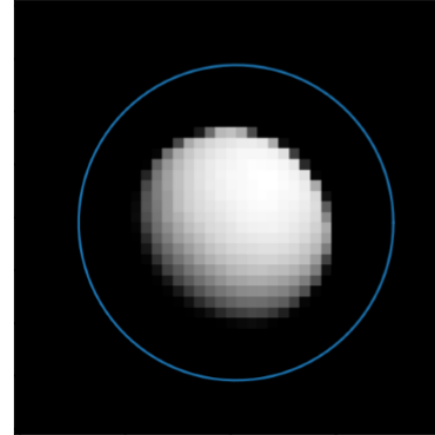


2. Overview of IASI moon acquisitions until now (3/4)

❖ For a central transit, example of a lunar IASI-C spectrum



Central (P) ✓



Due to the very few number of good lunar spectra available, a reduction of the noise is performed by averaging 30 consecutive wavenumbers ($30 \times 0.25 \text{ cm}^{-1} = 7.5 \text{ cm}^{-1}$)

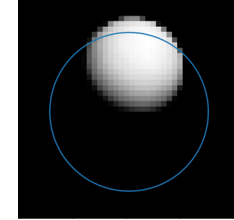
2. Overview of IASI moon acquisitions until now (4/4)

❖ But for other types of transits, some default appears :

1. Scene instability during interferogram acquisitions :

- View-steering is OFF during external calibration mode;
 - Moon moves in the FOV during interferogram acquisitions, so when it's not completely inside IASI pixel:
- ⇒ Leading to non symmetrical interferograms = problems for data processing

Partial (P) ≈



2. IASI IPSF (Instrument Point Spread Function) are spectrally dependent :

B1, B2 and B3 can see a scene slightly different at the same time because of very strong heterogeneity of the scene: hot Moon + cold space

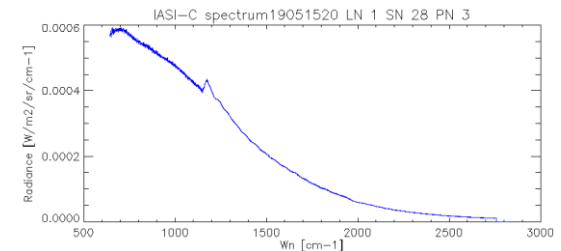
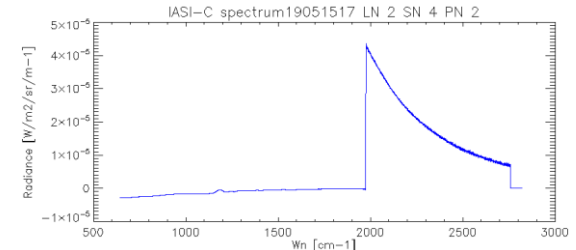


Example : loss of B1 + B2

3. The optical transmission at the interbands is very sharp : inducing an ISRF (Instrument Spectral Response Function) distortion at these wavenumbers.



Example : bad spectrum shape at the interbands



3. First phase of the Moon Study conclusions and recommendations (1/4)

❖ What was done during the first phase of the study in 2019 :

3.1 A precise model of moon radiances in the TIR domain has been developed for the study ≡

(1) Thermal emission of the lunar surface (Lunar surface T° derived from Diviner L4 cumulative GCP product and Lunar surface emissivity derived from Apollo Moon samples)

+ (2) Solar radiation reflected by the lunar surface (The distinction of soil type (for emissivity computation) is derived from the rock abundance of the LRO/Diviner product. The radiance is a function of time depending on the geometry between Sun-Earth-Moon and considering the Moon phase and the % of the illuminated surface)

+ (3) Earth radiation reflected by the lunar surface (negligeable)

⇒ Approximations of the model are identified and evaluated in term of sensitivity :

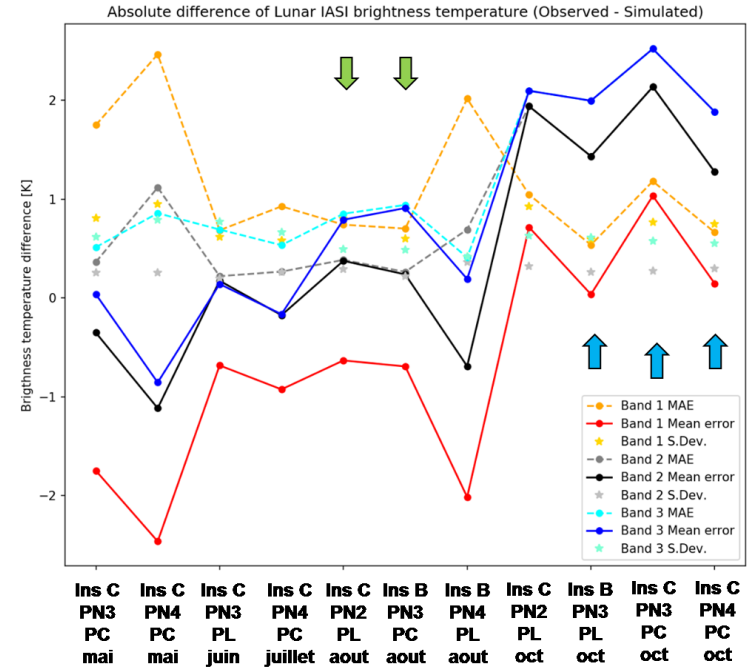
- Surface température (LRO/Diviner vs. Model Vasavada et al.) : landscape effect on T_{surface}
- Effect of Libration on Surface température (LRO/Diviner)
- Variability of solar constant (seasonal variability + solar activity) for solar radiation and for lunar surface temperature (via Vasavada et al. model)

3. First phase of the Moon Study conclusions and recommendations (1/4)

❖ What was done during the first phase of the study in 2019 :

3.2 Comparisons have been performed between the model and the mesured moon spectra

- ⇒ The obtained moon physical radiances from the model were convolved with IASI IPSF in order to compare them with the IASI L1C spectra
- ⇒ The relative position of the IPSF reference frame and the Moon model frame is determined by localizing the Moon in IIS images (during an orbit)
- ⇒ The difference is larger for October compare to August. Due to the size of the Moon (larger = more sensitive to IPSF uncertainties) ? ⇒ We need more data to answer



3. First phase of the Moon Study conclusions and recommendations (2/4)

❖ What was done during the first phase of the study in 2019 :

3.3 Highlights of too high uncertainties for geolocation and IASI IPSF for the radiometric model : (not a problem for classical IASI EW observations because of the calibration)

- ⇒ ✓ Yaw steering angle (platform compensation to follow earth rotation) : a systematic positive bias between minimised and theoretical values ⇒ Corrections applied for the study are satisfactory in terms of accuracy
- ⇒ ✓ Oscillations in Y & Z axis : not correlated between the 2 axis. Due to platform attitude oscillations?
⇒ Corrections applied for the study are satisfactory in terms of accuracy
- ⇒ ☹ IIS FOV : a more precise estimation method was developed = showed uncertainties more important than expected
- ⇒ ☹ IPSF weight between the 4 detectors (each pixel) of a same spectral band (uncertainties/variability of 2 or 3%)
⇒ Need to estimate the exact impact on the results, and pursue the study on this point

3.4 Inter-pixels mono-transit analysis shows some systematic biases (exemple for PN3 and PN4 of IASI-C)

⇒ could be caused by IPSF weight

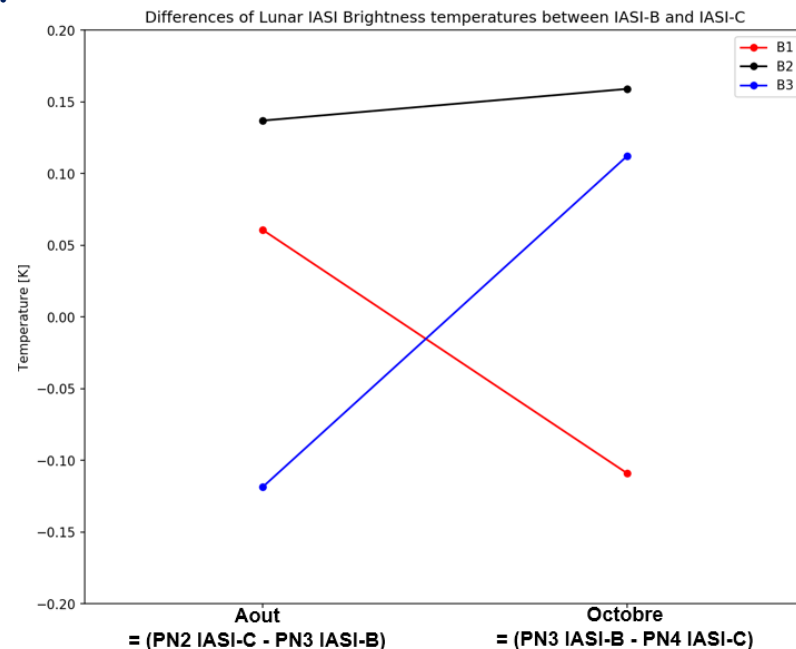
	PN3(C) - PN4(C) Mai 2019 IASI-C	PN3(C) - PN4(C) October 2019 IASI-C
SB1	0,72 K	0,89 K
SB2	0,76 K	0,86 K
SB3	0,89 K	0,64 K

3. First phase of the Moon Study conclusions and recommendations (3/4)

❖ What was done during the first phase of the study in 2019 :

3.5 Inter-comprisons analysis between two different instruments : IASI-B and IASI-C

- ⇒ Only 2 transits : in August PN3 IASI-B vs PN2 IASI-C + October : PN3 IASI-B vs PN4 IASI-C
- ⇒ Comparison always between a central transit (C) and a bordering transit (L)
- ⇒ For the 3 bands, the differences are lower than the differences between the pixels of the same instrument (ex PN3/4 IASI-C) : radiance difference ≤ 0.2 K (so ≤ 0.4 %).
- ⇒ But the comparison is very reduced (only 2 points)
 - ⇒ we need more data to consolidate the results.



Difference of Lunar IASI Brightness Temperature between IASI-B and IASI-C in K

3. First phase of the Moon Study conclusions and recommendations (4/4)

❖ Conclusion of the first phase of the study in 2019 :

- The potential of the Moon for IASI absolute calibration and relative inter-comparison have been evaluated for the first time. The radiometric model could be used for other TIR missions (IASI-NG, CRIS).
- The results are promising and can be improved:
 - For **absolute** calibration using the Moon, the reached accuracy is $1 - 2 \text{ K}$ (absolute brightness temperature)
 - For **relative** calibration (inter-instrument), the accuracy is $\leq 0.15 \text{ K}$... but we have only 2 transits

BUT the amount of available data limits the extent of this conclusion.

More data are needed to consolidate the results and improve the radiometric model

- ⇒ The 'central' pixel passages are the best data. The first study used also the 'nearly central' passages, but the amount of available data did not permit us to conclude if those passages are 'safe' to be used;
- ⇒ Analyse more precisely the inter-pixel variations due to the detector;
- ⇒ A longer time-series of Moon acquisitions is essential to understand the results variabilities (IPSF sensitivity, phase of the Moon);
- ⇒ Consolidate the spectral emissivity data ⇒ better estimation of the moon surface temperature with IASI larger spectral coverage than Diviner
- ⇒ The study permitted to characterize independently some parameters of the IASI system (IIS FOV, IPSF size and weights, oscillations of the platform, yaw steering) and showed non negligible and interesting uncertainties on these parameters
⇒ **with more data the absolute calibration using the moon will reach a better accuracy**

4. IASI moon acquisitions constraints

Here is the list of IASI moon acquisitions operational constraints which the CNES IASI team have to deal with

4.1 The replacement of the Cold Space coding table by the Moon coding table :

⇒ The new Moon coding table doesn't have the same dynamic than the cold space coding table which was used before for the monitoring of the scan mirror reflectivity over time (monitored every month until now and updated \approx every 1 year and half). This monitoring is critical for the IASI radiometric error performance.

4.2 Moon CS2 external calibration planning on 2 instruments for 1 year and minimise the outage for the users

⇒ Data availability for users is an important matter = important organisation was pulled off to reduce the external calibration routine amount to once per quarter (instead of once per month);

⇒ We organised a IASI operation calendar covering 15 months for IASI-B and IASI-C with respect to IASI EUMETSAT team constraints (conf delivery, updates, decontamination, routine ext cal, Moon acquisitions, ...) to minimize as much as possible the operations and still ensure a sufficient monitoring;

4.3 OPS dedicated reprocessing at CNES for decoding Moon spectra :

⇒ The OPS configuration is only adapted to EW spectra retrievals. The IASITEC team at CNES has to reprocess each time the data with a dedicated configuration.



5. Conclusion and upcoming program for the next phase of the study in 2021

- ❖ The scientific community and the GSICS are really interested in this work for the TIR domain:
(from last GSICS meeting) R.GIR.20200319.1: CNES to consider making further lunar acquisitions with IASI to extend their valuable analysis of the potential of this technique and share with the lunar calibration community.
- ❖ At the IASI REVEX in July 2020, everyone was in agreement to pursue the Moon study with a year of Moon acquisitions on IASI-B and IASI-C from January 2021 to December 2021.
Moon acquisitions are planned once a month when its phase is at its maximum.

THANK YOU EVERYONE

BACK-UP SLIDES

Radiometric model (1/10)

❖ A precise model of moon radiances in the thermal infrared domain has been developed for the study

❖ Lunar radiances are composed of 3 components : $L_{Moon} = L_{eMoon}^{(1)} + L_{rSun}^{(2)} + L_{rEarth}^{(3)}$

(1) Thermal emission of the lunar surface:

$$L_{eMoon}(\lambda) = \epsilon(\lambda) B(\lambda, T_{Moon})$$

(2) Solar radiation reflected by the lunar surface:

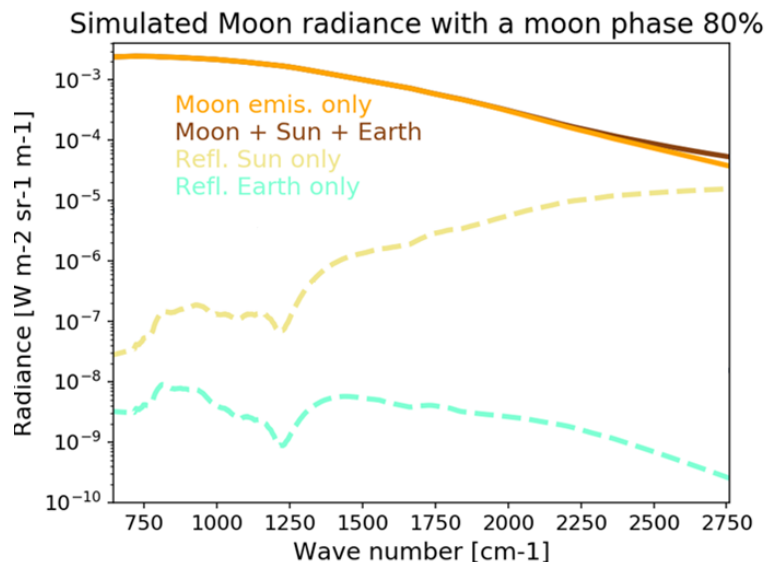
⇒ Important in SWIR domain

$$L_{rSun}(\lambda) = \pi F_{SunIN}(\lambda) \cdot r_{Moon}(\lambda)$$

(3) Earth radiation reflected by the lunar surface:

⇒ negligible

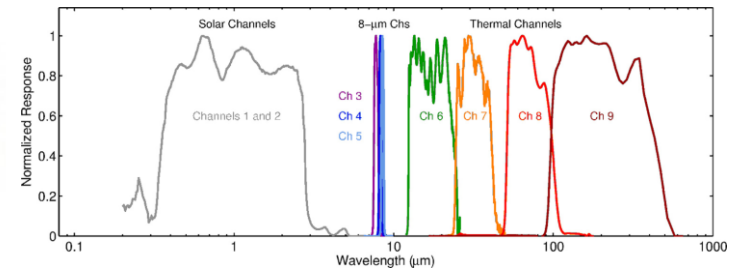
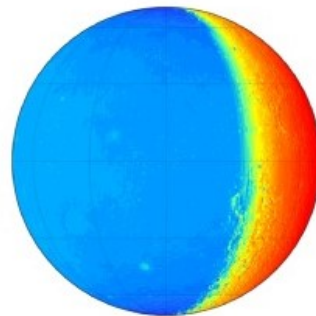
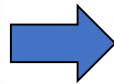
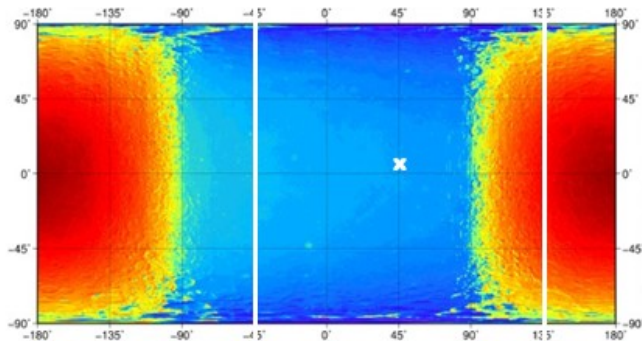
$$L_{rEarth} = \pi F_{EarthIN}(\lambda) \cdot (1 - \epsilon(\lambda))$$



Radiometric model (2/10)

❖ Parameters of the model:

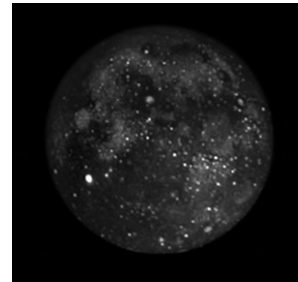
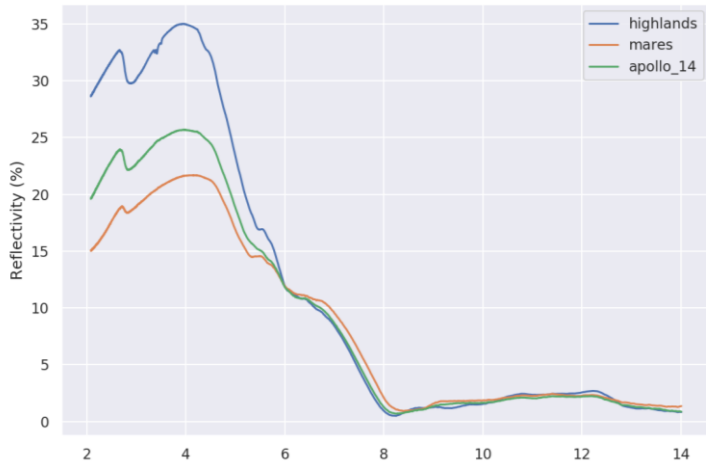
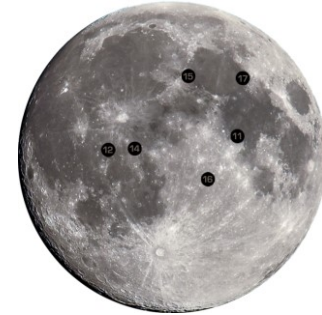
- ✓ **Lunar surface temperature** derived from Diviner L4 cumulative GCP product
- ⇒ Diviner is a multiband radiometer (2 solar channels, 7 channels from 7.5 to 400 μm) on-board Lunar Reconnaissance Orbiter (LRO), JPL. Launched on 2009 and still operational, continuous acquisitions.
- ⇒ Diviner lunar surface temperature $f_n(\text{lon}, \text{lat}, t)$ are at the state of the art, resulting of the processing of measurements from 2009 to 2015.
- ⇒ Spatial resolution: 0.5° ; temporal : 0.25h lunar.
- ⇒ These data have been processed for our purpose and all the geometry defined.



Radiometric model (3/10)

❖ Parameters of the model:

- ✓ **Lunar surface emissivity** derived from Apollo Moon samples
- ⇒ available in ECOSTRESS (ASTER) database for Apollo 11, 12, 14 and 16 (Salisbury et al. 1997)
- ⇒ Emissivity spectral properties are dependant of the surface type, especially @ $\lambda < 6 \mu\text{m}$
 - Apollo 11, 12 – Maria (lunar oceans): « Young soil », darker
 - Apollo 16, (14) – Highlands: « Old soil », brighter
 - Apollo 14 – Transitional case



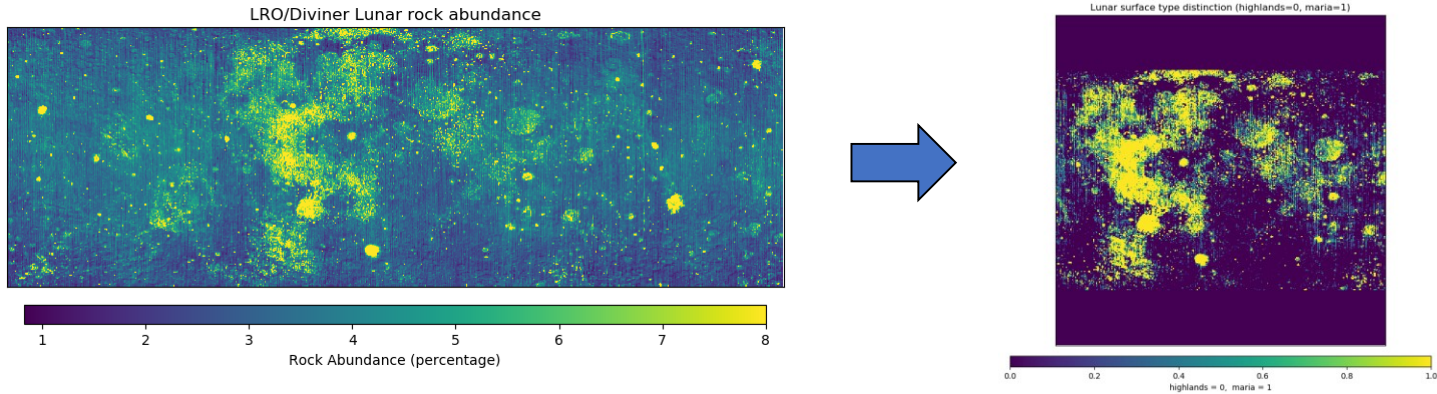
Moon @ $3-5 \mu\text{m}$ during eclipse

- ✓ Hot-spots are recent craters
- ✓ We have to distinguish highlands vs maria + craters

Radiometric model (4/10)

❖ Parameters of the model:

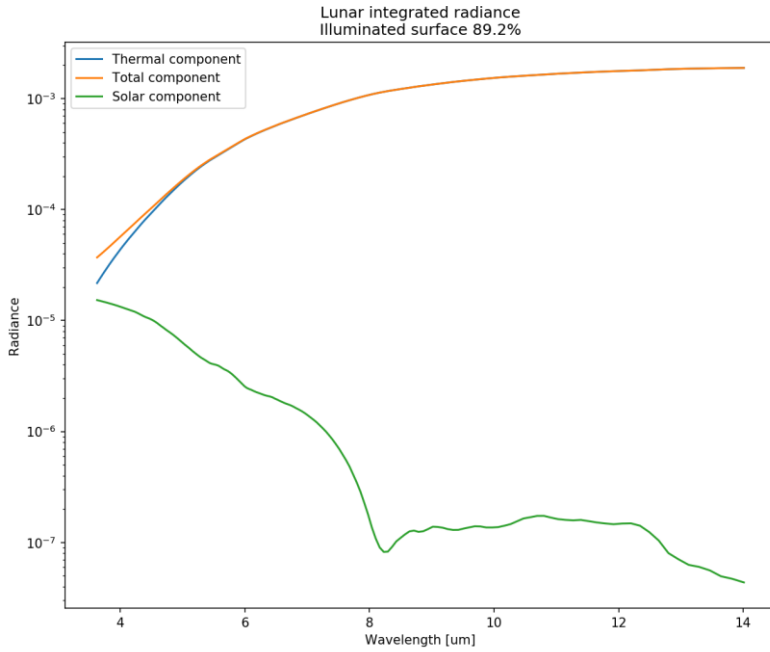
The distinction of soil type (for emissivity computation) is derived from the rock abundance of the LRO/Diviner product



- ✓ **Solar radiation** reflected by the lunar surface is computed with these hypotheses:
- ⇒ The sun is considered as a blackbody with $T=5780$ K
- ⇒ Radiance is a **function of time**, depending on the geometry between Sun-Earth-Moon
- ⇒ Moon phase and the % of the illuminated surface

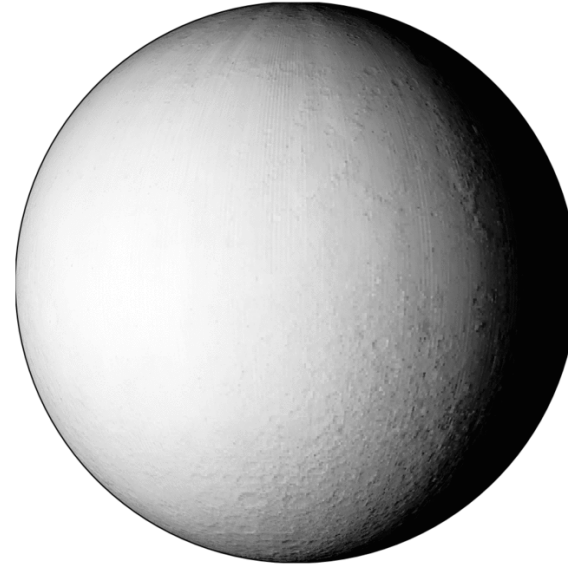
Radiometric model (5/10)

❖ Moon radiance simulated by the model



Total component of the Moon Radiance @ 14μm
Illuminated Moon surface 89.2%

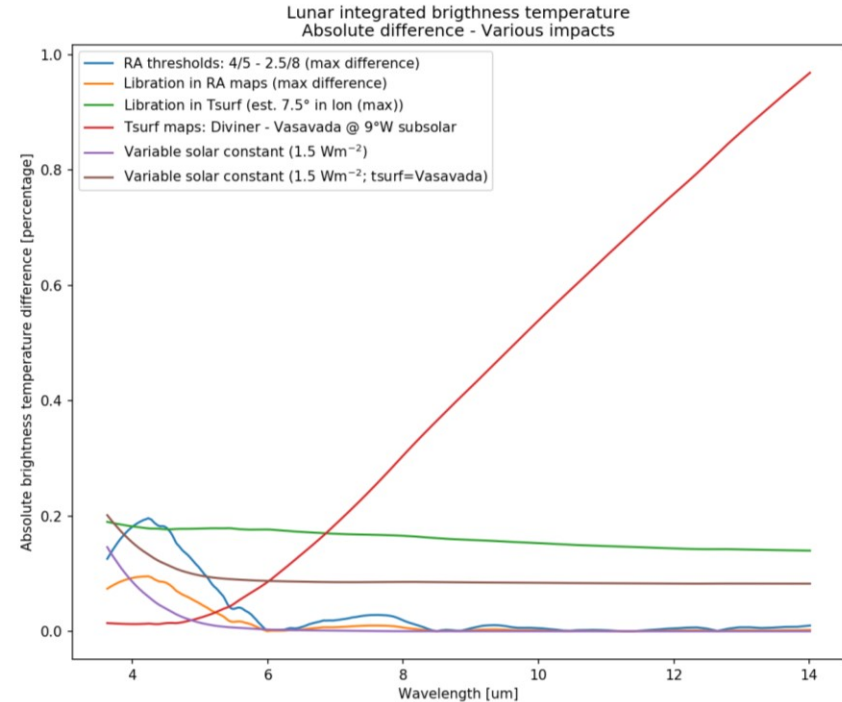
$$\left[\frac{W}{m^2 sr m^{-1}} \right]$$



Radiometric model (6/10)

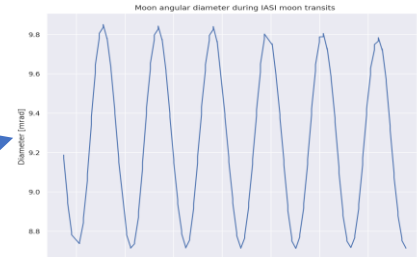
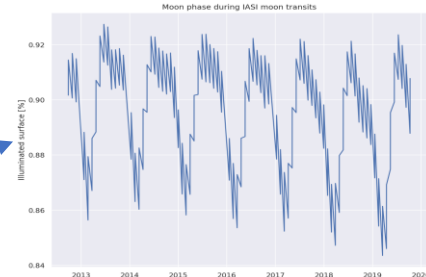
❖ Approximations of the model are identified and evaluated in term of sensitivity in the model by taking the maximum amplitude

- ✓ Surface température (LRO/Diviner vs. Model Vasavada et al.): (landscape effect on Tsurf)
 - ✓ Effect of Libration on Surface température (LRO/Diviner)
 - ✓ Effect of Libration on Libration rock abundance (LRO/Diviner): very low \Rightarrow libration not taken into account in the model
 - ✓ Thresholds on Rock abundance for surface types
 - ✓ Variability of solar constant (seasonal variability + solar activity) for solar radiation and for lunar surface temperature (via Vasavada et al. model)
- Good confidence in the model and the choices made



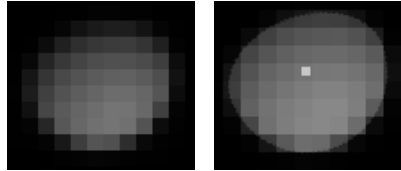
Radiometric model (7/10)

- ❖ The model was used to compute **the variation of lunar radiances** in time seen by a IASI instrument over a long period: from launch (2012) to now, representing ≈ 390 transits with Moon phase ≈ 0.9
- ❖ The **moon phases** seen in IASI CS2 view:
 - ⇒ Close to Full Moon: 83-94%
 - ⇒ Between 2 successive orbits (101min), the Moon phase changes $\sim 0.4\%$
 - ⇒ Close to New Moon: 6-17%
- ❖ The **moon diameter** in IASI FOV: from 35.2% to 46.1%
 - ⇒ For IASI-B (this graph): 8.71 to 9.85 mrad
 - ⇒ Between 2 successive orbits (101min), the Moon diameter changes $\sim 0.2 \mu\text{rad}$
- ❖ Combining the variation of phase and diameter of the Moon seen by IASI-B, we obtain the variation of The **lunar radiance** seen by IASI: from ~ 9 to $\sim 13.5\%$
 - ⇒ Between 2 successive orbits (101min), the lunar radiance changes $\sim 1\%$

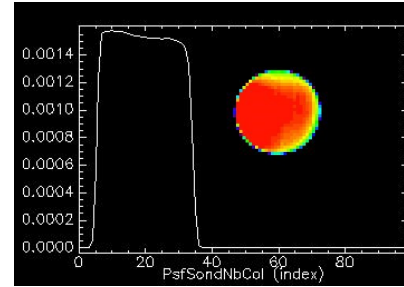


Radiometric model (8/10)

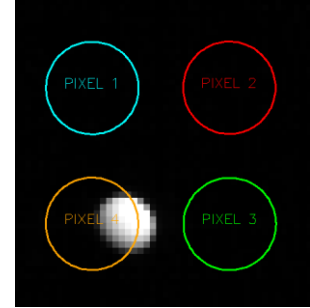
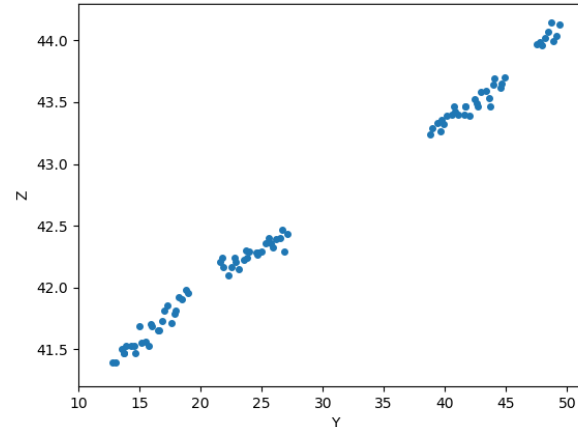
- ❖ Physical radiances of the Moon computed by the model are then convolved with IASI IPSF in order to compare them with the IASI L1C measurements.
 - ❖ The relative position of the IPSF reference frame and the Moon model frame is determined by localizing the Moon in IIS images.
 - ❖ Several approaches were tested, the better one process IIS images, by comparing a synthetic image with the measured one
- ⇒ Accuracy ≈ 0.25 IIS pixel



- ❖ Positions of the center of the Moon in IIS coordinates are obtained for one orbit with several Moon transits in CS2

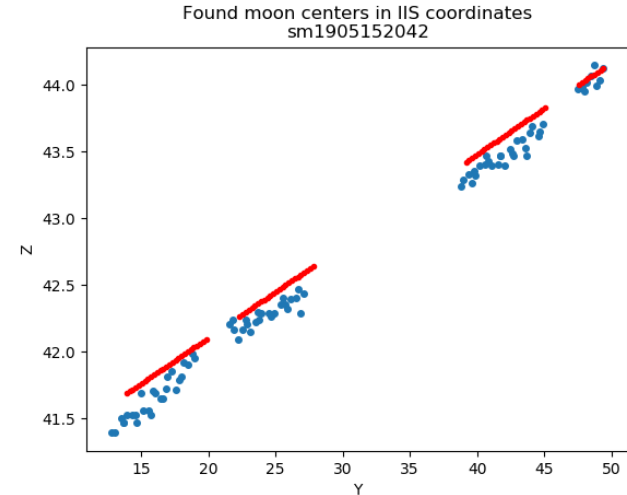
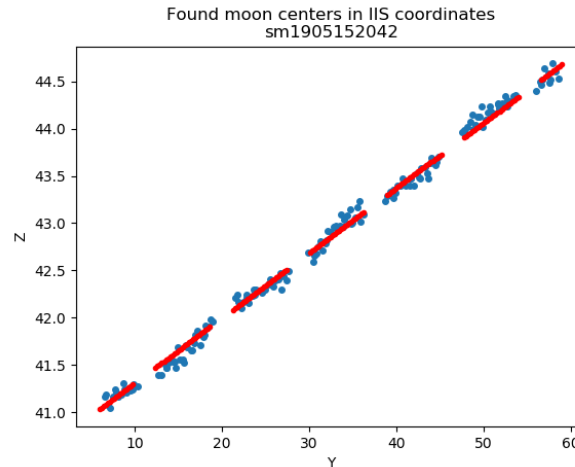


Found moon centers in IIS coordinates
sm1905152042



Radiometric model (9/10)

- ❖ Moon trajectory in IIS FOV is supposed to be a straight line, the slope being the yaw steering compensation angle. Knowing the acquisition time IIS and the Moon speed in IIS FOV, the Moon positions in IIS images are simulated and compared to the one previously retrieved.
- ❖ The differences being large, a minimisation of the distance between synthetic positions and computed ones is done, by adjusting these parameters:
 - ⇒ Initial synthetic positions
 - ⇒ FOV IIS size
 - ⇒ Yaw steering angle
- ❖ After minimisation:
 - ⇒ Some oscillations are visible



Radiometric model (10/10)

❖ We thus add these parameters in the minimisation:

⇒ Amplitude, period and offset of Z axis oscillations

⇒ Amplitude, period and offset of Y axis oscillations

❖ This minimisation highlighted an uncertainty too large of some parameters:

❖ IIS FOV in IASI L1 ground configurations : 62.72 mrad

(specification: $59.63 \text{ mrad} \leq \text{FOV} \leq 62.53 \text{ mrad}$)

⇒ deduced for IASI-C (7 orbits): $61.15 \pm 0.12 \text{ mrad}$

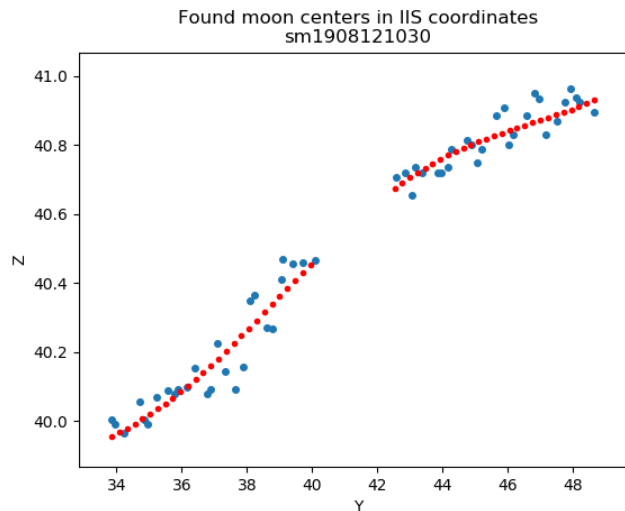
⇒ deduced for IASI-B (3 orbits): $60.73 \pm 0.04 \text{ mrad}$

❖ Yaw steering angle: a systematic positive bias between minimised and theoretical values of $0.1^\circ \pm 0.024^\circ$

⇒ Can be explained by MetOp pointing knowledge (0.07° (x-axis), 0.10° (y-axis), 0.17° (z-axis)) or a rotation of IIS FOV of 0.1°

❖ Oscillations in Y & Z axis

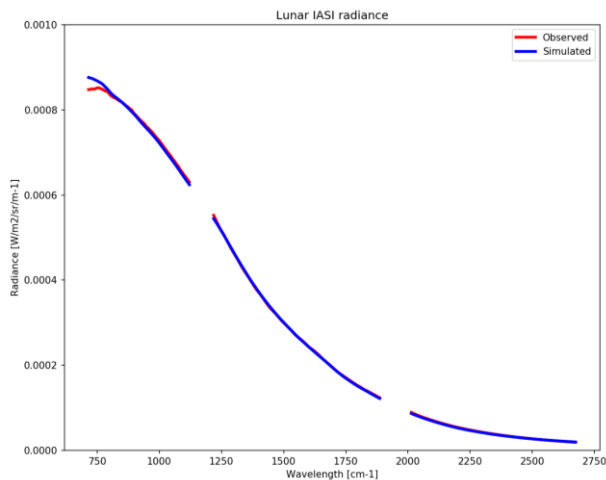
⇒ Not correlated between the 2 axis, amplitude varies in time. Probably due to MetOp attitude oscillations ?



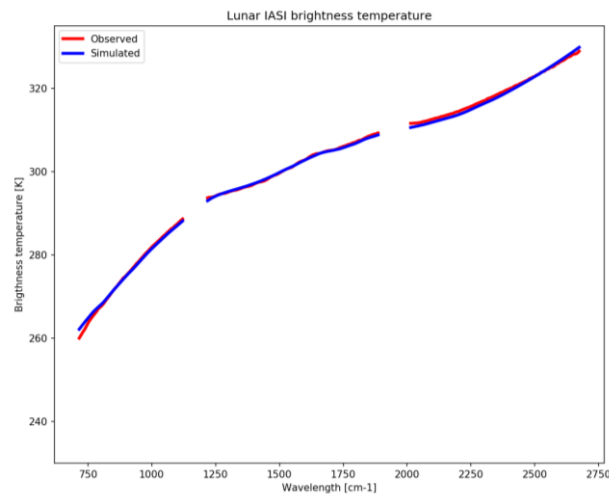
Inter-comparisons analysis (1/10)

❖ Comparison between simulation and observations

❖ Example in radiance



In Brightness temperature

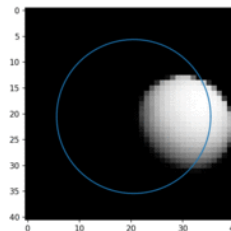


❖ The Moon is covering only a part of IASI pixel, so the non-linearity conversion in brightness temperature induce a different temperature for the 3 bands:

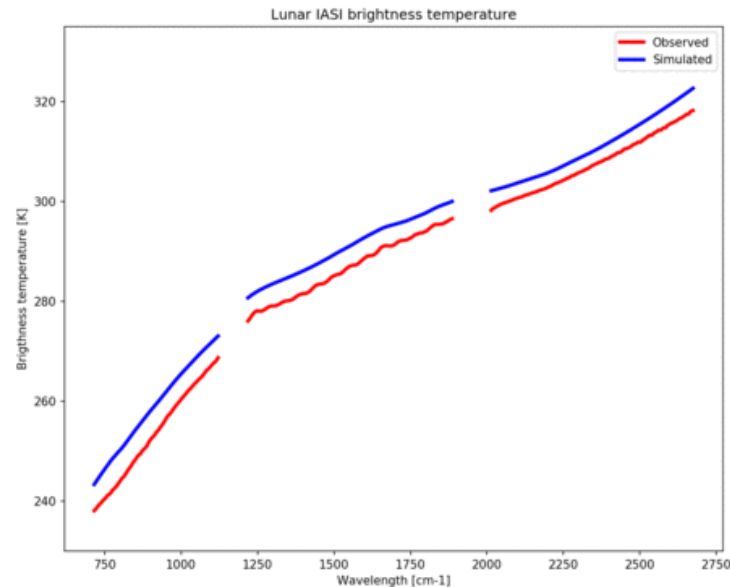
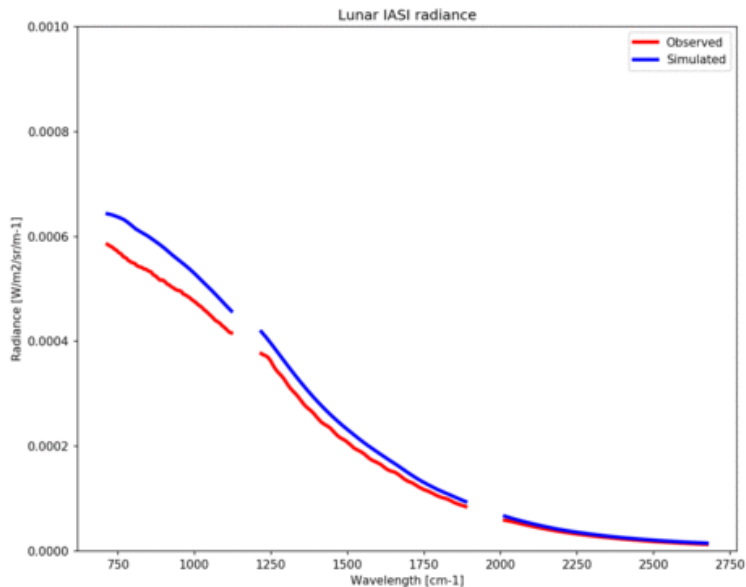
- B1 : ~ 280 K
- B2 : ~ 300 K
- B3 : ~ 320 K

Inter-comparisons analysis (2/10)

- ❖ Example of a Moon transit
- ❖ Radiance

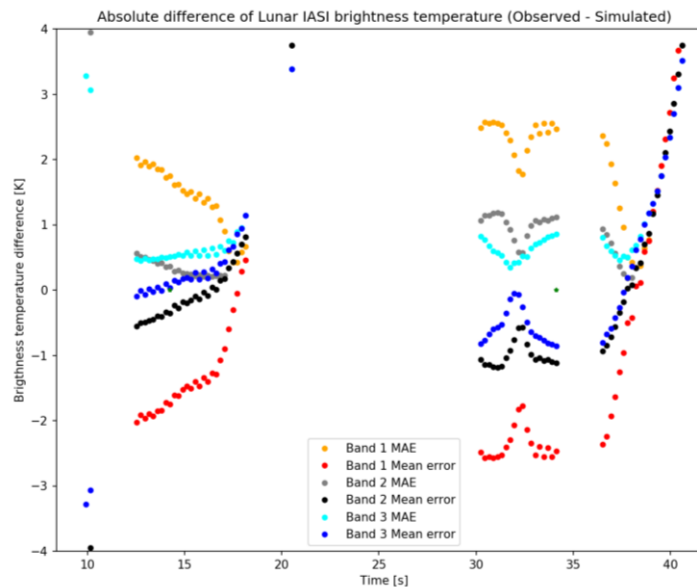
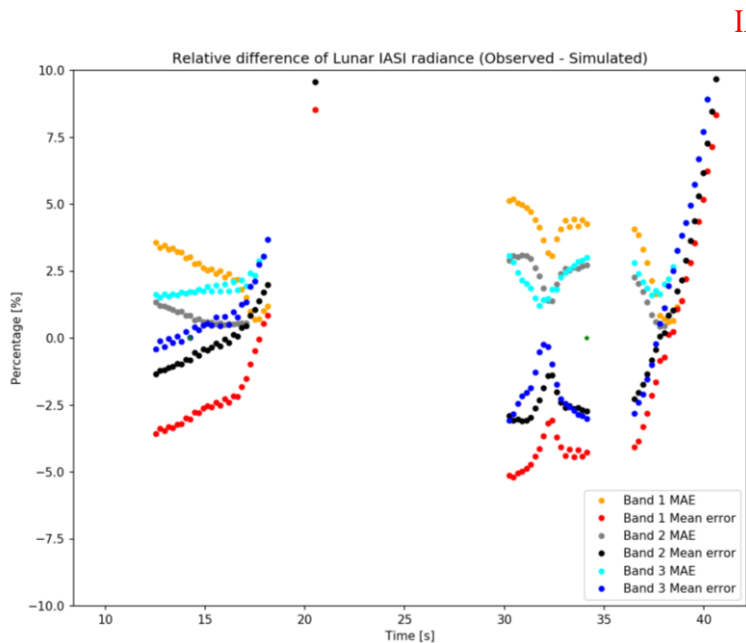


Brightness Temperature

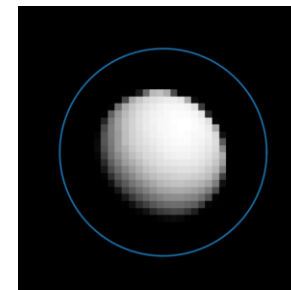


Inter-comparisons analysis (3/10)

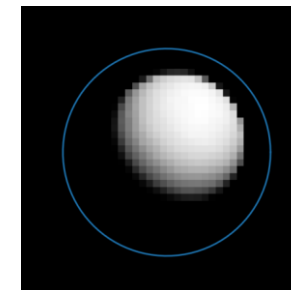
- ❖ Relative difference : changes of Moon diameter and phase is normalized between the different transits
- ❖ Evolution of the difference (observed – simulated) in relative radiance and ΔT_b per band for **May 2019**



PN3



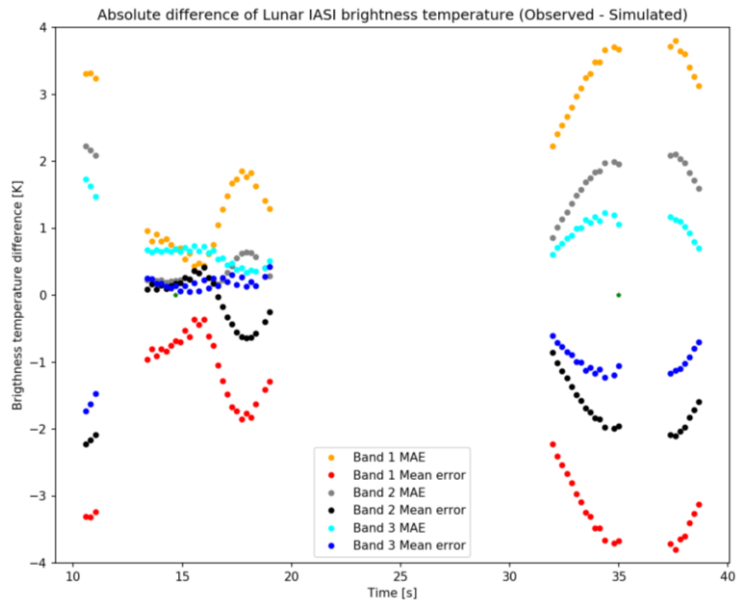
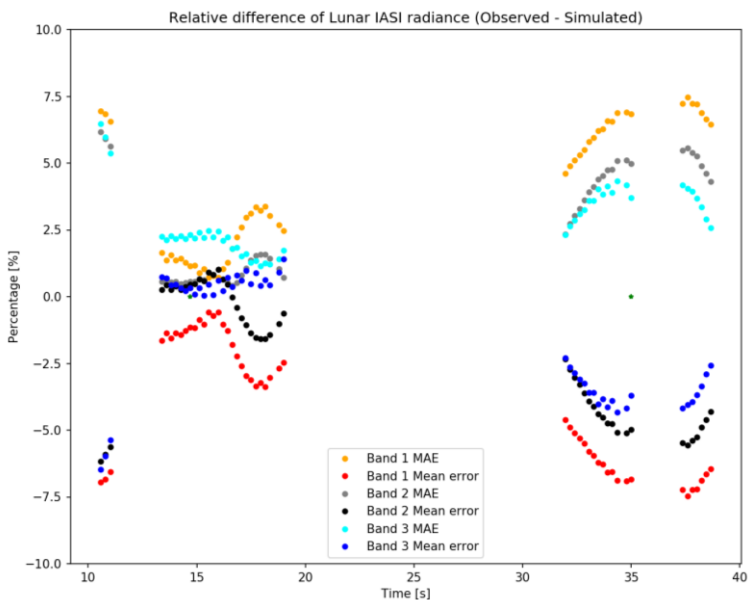
PN4



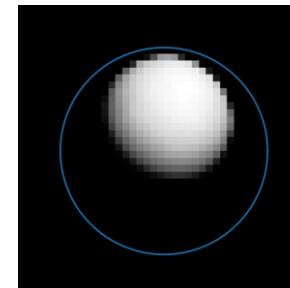
Inter-comparisons analysis (4/10)

❖ Evolution of the difference (observed – simulated) in relative radiance and ΔT_b per band for June 2019

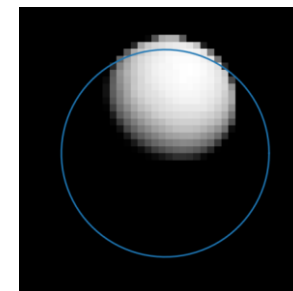
IASI-C



PN3



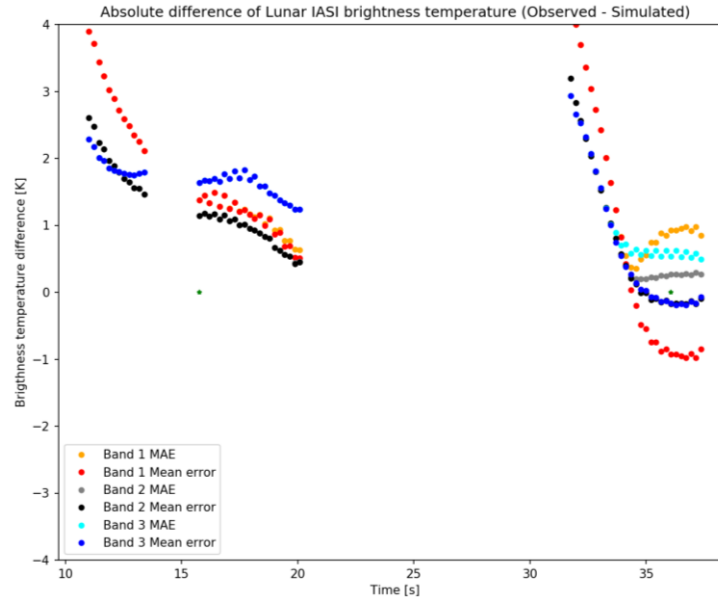
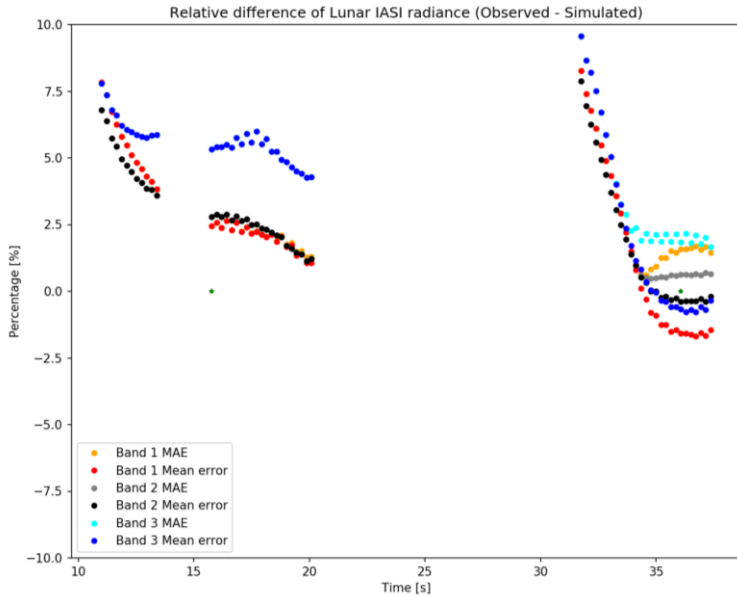
PN4



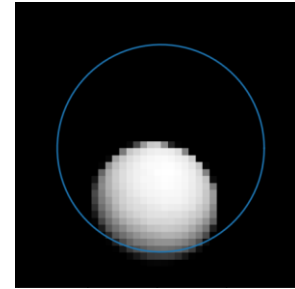
Inter-comparisons analysis (5/10)

❖ Evolution of the difference (observed – simulated) in relative radiance and ΔT_b per band for July 2019

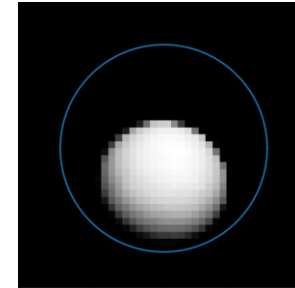
IASI-C



PN3



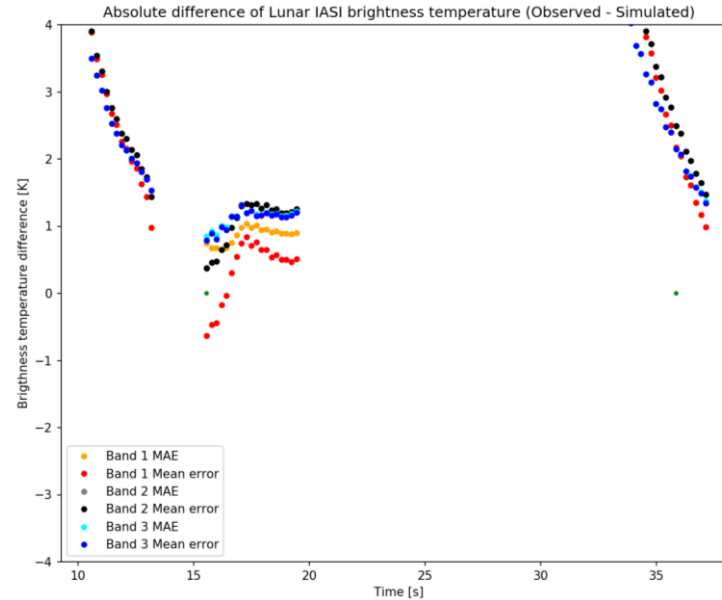
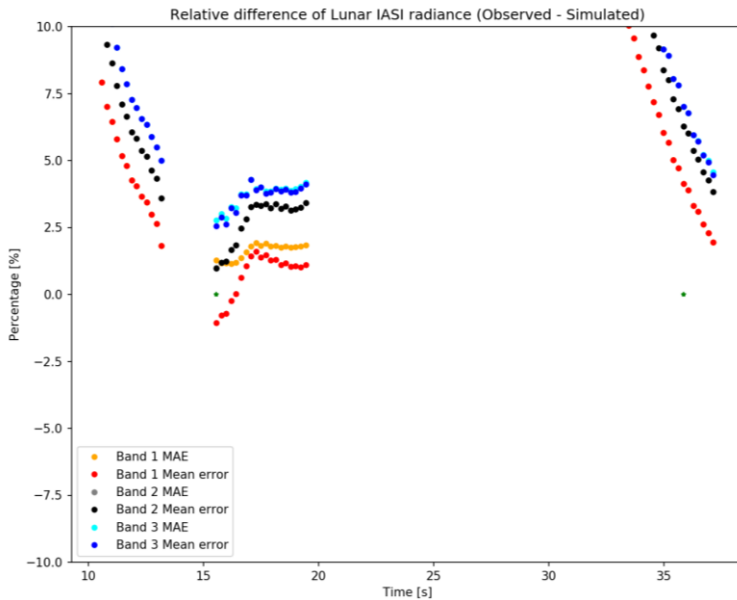
PN4



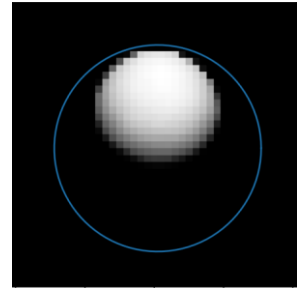
Inter-comparisons analysis (6/10)

- ❖ Evolution of the difference (observed – simulated) in relative radiance and ΔT_b per band for August 2019

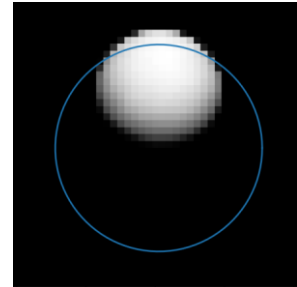
IASI-C



PN2



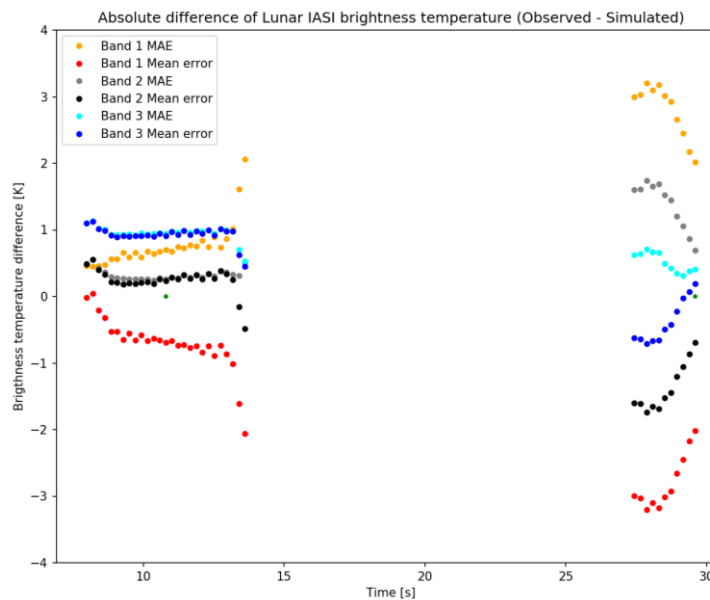
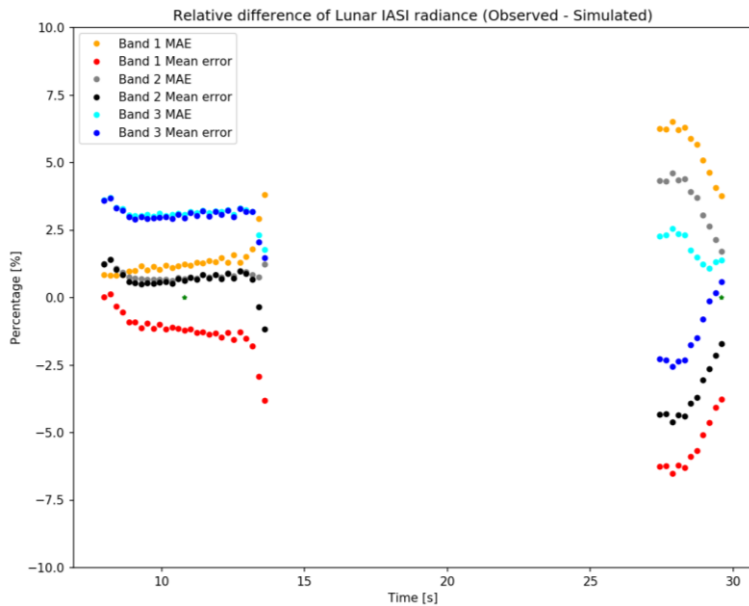
PN1



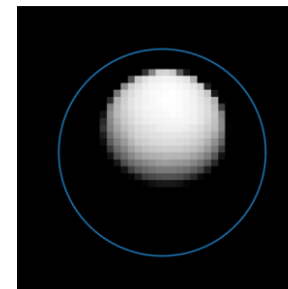
Inter-comparisons analysis (7/10)

- Evolution of the difference (observed – simulated) in relative radiance and ΔT_b per band for August 2019

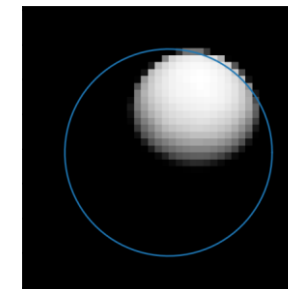
IASI-B



PN3



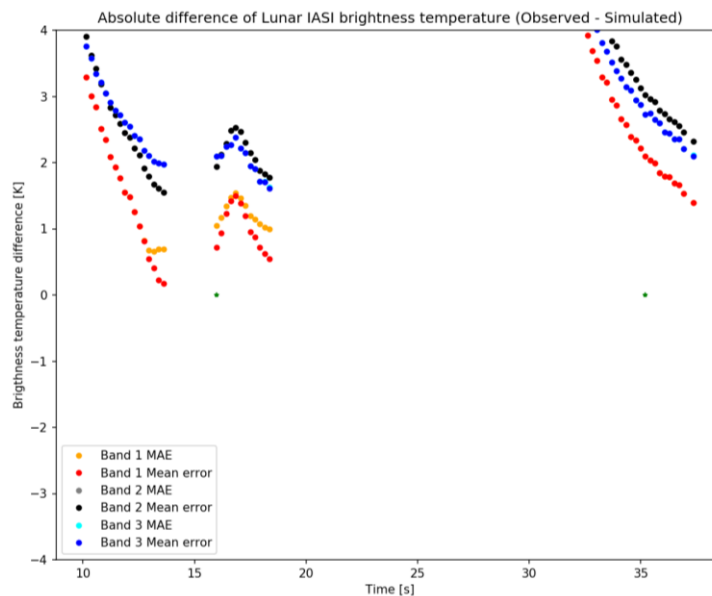
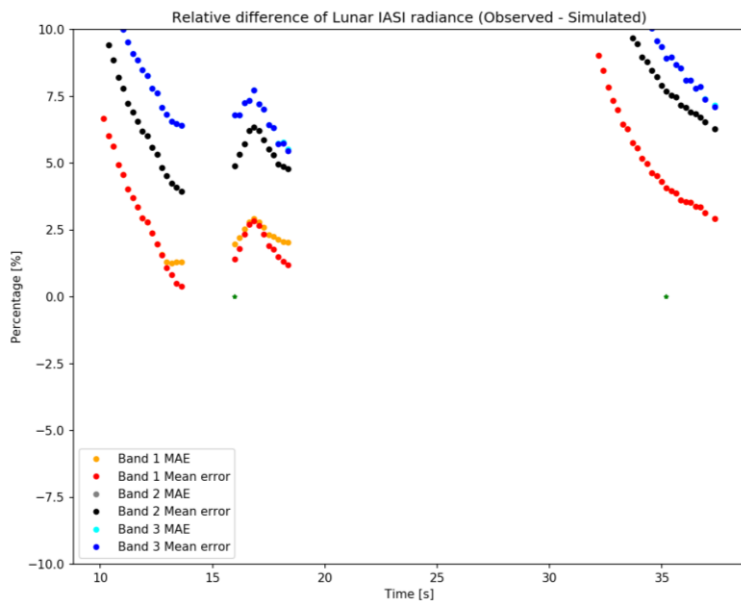
PN4



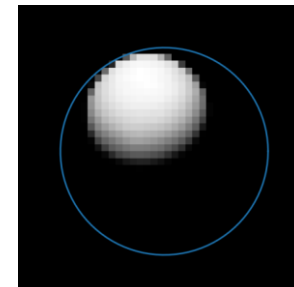
Inter-comparisons analysis (8/10)

- Evolution of the difference (observed – simulated) in relative radiance and ΔT_b per band for **October 2019**

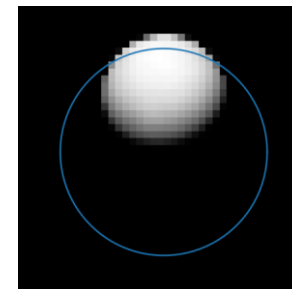
IASI-C (1/2)



PN2



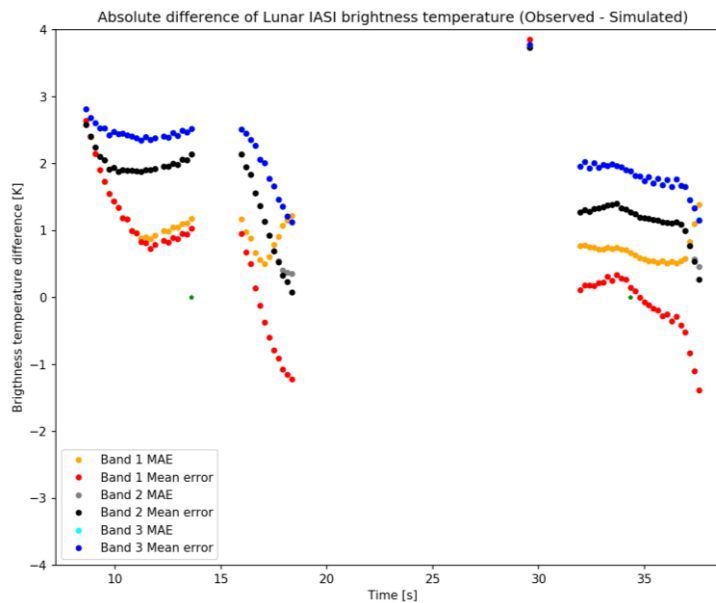
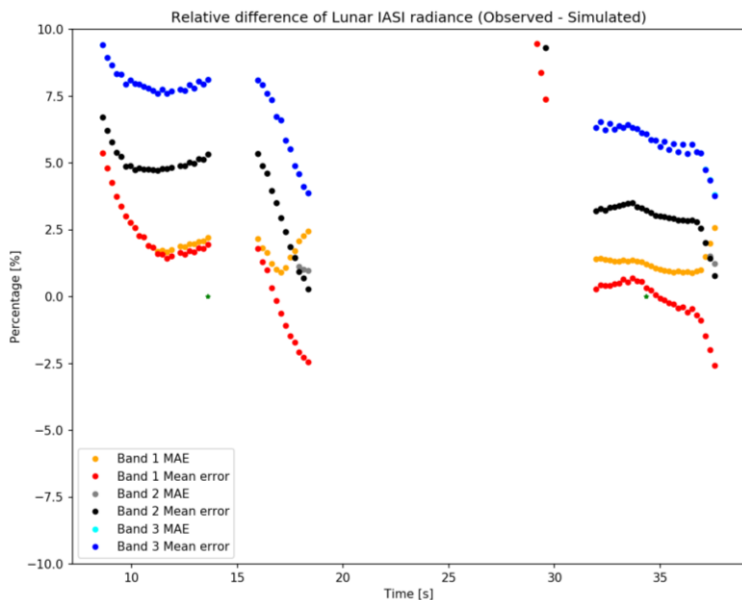
PN1



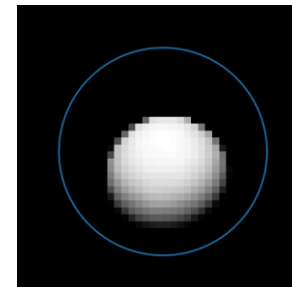
Inter-comparisons analysis (9/10)

❖ Evolution of the difference (observed – simulated) in relative radiance and ΔT_b per band for **October 2019**

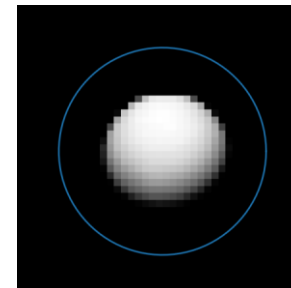
IASI-C (2/2)



PN3



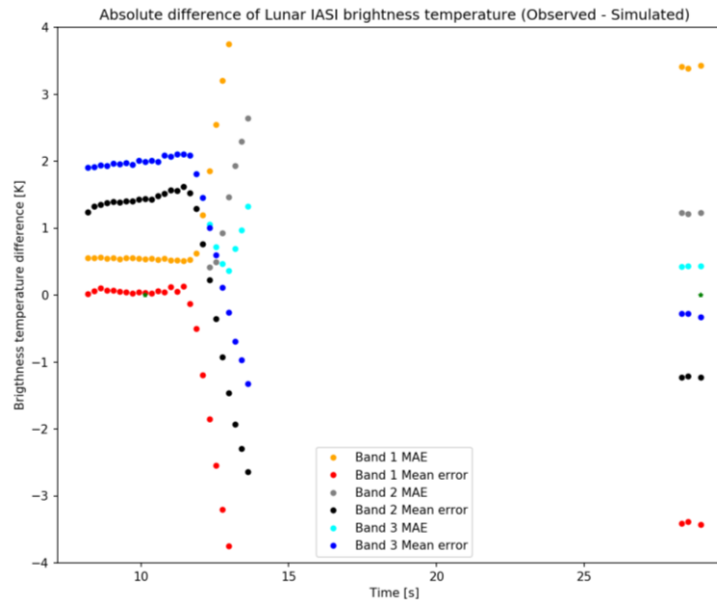
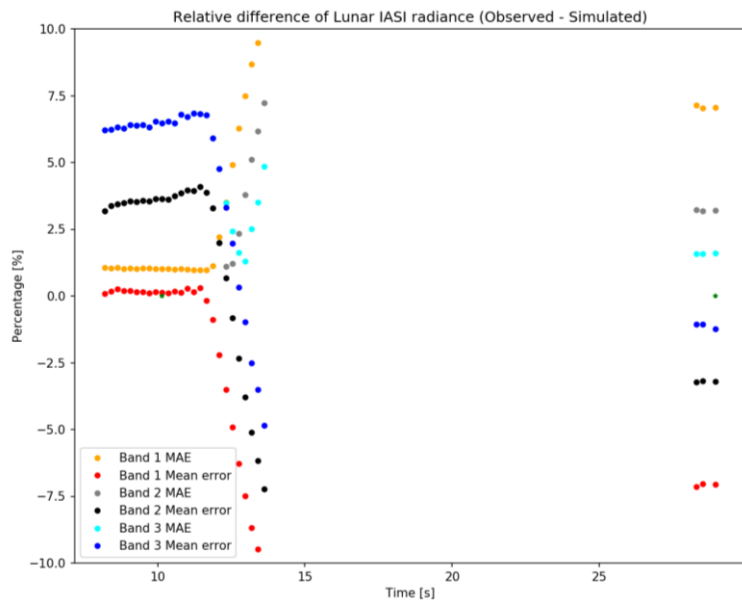
PN4



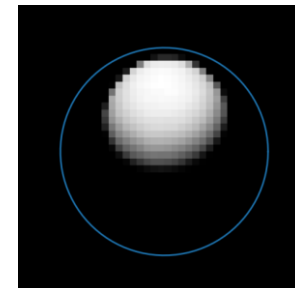
Inter-comparisons analysis (10/10)

- ❖ Evolution of the difference (observed – simulated) in relative radiance and ΔT_b per band for **October 2019**

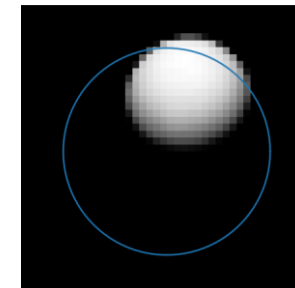
IASI-B



PN3



PN4



Overview of IASI moon acquisitions until now

❖ Data available for the study

IASI-C

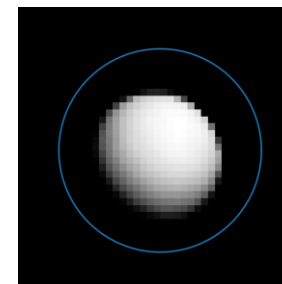
Date	Instrument	Pixel / Type de passage (C - central, P - partiel, L - limitrophe)	Phase (pourcentage de la surface illuminée)	Diamètre de la Lune (mrad)
201906141200	IASI-C	PN3/PN4 L/P	91.1 %	9.322
201908120815	IASI-C	PN2/PN1 L/P	91.1 %	8.890
201910101257	IASI-C	PN3/PN4 C/C	90.3 %	8.713

IASI-B

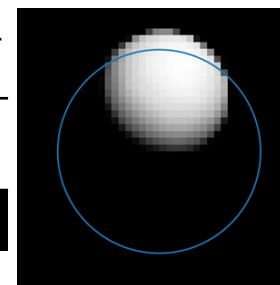
Date	Instrument	Pixel / Type de passage (C - central, P - partiel, L - limitrophe)	Phase (pourcentage de la surface illuminée)	Diamètre de la Lune (mrad)
201910101151	IASI-B	PN3/PN4 P/L	90.0 %	8.714

Different types of moon transit inside IASI pixel

Central (C)



Partial (P)



Bordering (L)

